Exceptional Points in Plasmonic Waveguides Do Not Require Gain or Loss

Sung Yoon Min,[1] Ju Young Kim,[1] Sunkyu Yu,[2] Sergey G. Menabde,[1,*] and Min Seok Jang[1,†]

[1] *School of Electrical Engineering, Korea Advanced Institute of Science and Technology, Daejeon 34141, Korea*

[2] *Department of Electrical and Computer Engineering, Seoul National University, Seoul 08826, Korea*

(Received 6 May 2020; revised 11 August 2020; accepted 5 October 2020; published 17 November 2020)

Exceptional points (EPs) in photonics are associated with non-Hermitian Hamiltonians with energy gain or loss, a notable example is EPs in parity-time symmetric Hamiltonians. We show that, counterintuitively, actual energy gain or loss is not required to generate this type of non-Hermitian degeneracy, since the eigenvalue of the optical Hamiltonian is the mode's propagation constant and not the energy. This is demonstrated by a simple three-layer insulator-metal-insulator (I-M-I) plasmonic waveguide, the eigenmodes of which are known to experience degeneracy at a certain point in the parametric space suggested to be used for rainbow trapping. We identify this point to be, in fact, an EP with the coalescence of the eigenmodes, despite the system having neither parity nor time symmetry. Furthermore, we demonstrate the manifestation of a third-order EP, which is generated by merging two separate EPs in the parametric space of the I-M-I waveguide. The presented results reveal unconventional properties of the Hamiltonian of a simple plasmonic waveguide and provide an insight into the nature of EPs in non-Hermitian plasmonic systems in general, suggesting the possibility of accessing even higher-order EP regimes in simple photonic structures without the need for optical gain or loss.

DOI: 10.1103/PhysRevApplied.14.054041

I. INTRODUCTION

Non-Hermitian Hamiltonians with complex eigenvalues are widely used to describe physical systems with energy exchange, opposite to Hermitian Hamiltonians that signify ideal systems with energy conservation and real eigenvalues. However, non-Hermitian Hamiltonians possess much richer physics that was only recently unmasked. The groundbreaking study of Bender and Boettcher showed that even systems described by non-Hermitian Hamiltonians could exhibit real eigenvalues if the parity-time (PT) symmetry was satisfied [1]. These interesting notions of PT symmetry have been recently embraced by the field of photonics [2], where several optically coupled subsystems can exhibit gain or loss. In such photonic systems, the transition from real to complex eigenvalues at the exceptional point (EP) can be observed, depending on the interplay between the gain-loss and the coupling strength between the eigenmodes of the subsystems. The operation regime near the EP allows for the observation of intriguing phenomena, such as single-mode lasing [3,4], light trapping [5], and unidirectional invisibility [6,7].

Most of the photonic systems exhibiting EPs are realized by balancing the gain and loss of the constituent materials, which limits their practicality. To circumvent this issue, EPs in optical systems with structurally broken PT symmetry have been actively studied. For example, systems with an asymmetric loss-only configuration, which is a gauge-transformed PT-symmetric system, possess EPs forming at the transition between the states with complex eigenvalues [8]. Other works utilize radiation loss instead of material loss [9], exploiting their mathematical equivalence in the optical Hamiltonian. Nevertheless, all optical EPs that have been realized so far require energy exchange with outer systems.

Here, we reveal the possibility of exhibiting an EP in optical systems with neither energy gain nor loss, where the propagation constant is real at the EP. We argue that, unlike many quantum-mechanical and optical systems with energy as their eigenvalues, the Hermiticity of optical Hamiltonians for guided modes in waveguides is not directly related to energy conservation, as their eigenvalues are propagation constants of optical modes. As a representative example, we investigate lossless I-M-I plasmonic waveguides. Here, the I-M-I waveguide has eigenvalues of its optical Hamiltonian transitioning from being purely real to becoming a pair of complex conjugates. This behavior is strikingly similar to that of conventional PT-symmetric systems with balanced gain and loss [10,11], even though each eigenmode does not experience actual gain nor loss, while being a plasmonic mode without radiative loss. We also show that the EP in this system is robust to both P and T symmetry breaking. Furthermore, we

*menabde@kaist.ac.kr
†jang.minseok@kaist.ac.kr

numerically demonstrate a third-order EP that is expected to have strong potential in sensor applications [12,13] by combining two EPs in the parametric space. Finally, we investigate asymmetric *I-M-I* structures with and without material gain and loss, and we numerically demonstrate the constant presence of the EP regime in all cases.

II. RESULTS AND DISCUSSION

A. Exceptional points in an *I-M-I* waveguide

We start by considering the general case of a two-level system. The generalized mathematical condition to form an EP in a non-Hermitian two-level system with the Hamiltonian $H = \begin{pmatrix} a & b \\ c & d \end{pmatrix}$ is given by [14] $(a-d)^2 + 4bc = 0$. This condition allows an EP to be formed even without PT symmetry [15]: when $\mathrm{Re}[a] = \mathrm{Re}[d]$, so that $a-d$ is purely imaginary, while $b = c^*$, or when $a-d$ is real and $b = -c^*$. In a system of coupled waveguides, a and d correspond to the propagation constants of the eigenmodes of the subsystems, while b and c correspond to their coupling coefficients [8,16]. For example, photonic systems with symmetric real propagation constants and asymmetric losses [8] or radiation modes [9], as well as PT-symmetric systems, where [17,18] $a = d^*$, correspond to the case with purely imaginary $a-d$ and $b = c^*$. The condition $b = c^*$ is generally satisfied in symmetric coupled waveguides [16], except for anti-PT-symmetric systems, where [19,20] $a = -d^*$ and $b = -c^*$. Therefore, most studies consider PT-symmetric systems with gain and/or loss, where $a-d$ is purely imaginary. However, it is difficult to achieve the stable existence of an EP in conventional gain-loss photonic systems because of the low efficiency, narrow bandwidth, and nonlinear instability of gain materials. The selection of proper materials is also very limited. To avoid these problems while accessing the EP regime, one may consider a plasmonic system with purely imaginary a and d, so that $a-d$ is always purely imaginary. The simple *I-M-I* plasmonic waveguide is a handy example of such a system. Figure 1(a) schematically depicts the *I-M-I* plasmonic waveguide comprised of the two *I-M* interfaces, with the semi-infinite insulator layers I_1 and I_2 (with dielectric permittivities $\varepsilon_{I1,2}$; $\mathrm{Re}[\varepsilon_{I1,2}] > 0$), and the metal core M ($\mathrm{Re}[\varepsilon_M] < 0$) of thickness α. Then, we define $\rho_j = |\mathrm{Re}[\varepsilon_{Ij}]/\mathrm{Re}[\varepsilon_M]|$ and $\gamma_j = \mathrm{Im}[\varepsilon_{Ij}]/\mathrm{Re}[\varepsilon_{Ij}]$; $j = 1,2$. The plasmonic dispersion relation for a single *I-M* interface is given by $\beta_{I\text{-}M} = k_0 n_{I\text{-}M} = \pm k_0\sqrt{\varepsilon_M\varepsilon_I/(\varepsilon_M+\varepsilon_I)}$, where $\beta_{I\text{-}M}$ and $n_{I\text{-}M}$ are the propagation constant and effective mode index of surface plasmon, respectively, and $k_0 = 2\pi/\lambda_0$ is the free-space wave number. The dispersion of the *I-M-I* waveguide is known to be [21,22]:

$$\left(1+\frac{\varepsilon_M\kappa_{I1}}{\varepsilon_{I1}\kappa_M}\right)\left(1+\frac{\varepsilon_M\kappa_{I2}}{\varepsilon_{I2}\kappa_M}\right) = \left(1-\frac{\varepsilon_M\kappa_{I1}}{\varepsilon_{I1}\kappa_M}\right)\left(1-\frac{\varepsilon_M\kappa_{I2}}{\varepsilon_{I2}\kappa_M}\right)e^{-2\alpha\kappa_M}, \tag{1}$$

where $\kappa_j = ik_{y,j} = \sqrt{\beta^2 - \varepsilon_j k_0^2}$ is the decay constant along the y axis, α is the metal core thickness, and β is the propagation constant of the *I-M-I* eigenmode in the x direction.

When $\rho_{1,2} = \rho > 1$ and the system has neither gain nor loss ($\gamma_{1,2} = 0$), the *I-M-I* waveguide can support two propagating TM_0 eigenmodes with even parity of the governing H_z field (see Fig. 5 in Appendix) and antiparallel energy velocity, while their phase velocity is of the same sign [23]. The energy velocity is given by $v_E = \int S_x dy / \int u dy$, where S_x is the x component of the Poynting vector, and u is the time-averaged energy density [24]. For convenience, we call the mode with positive v_E a forward mode, $|f\rangle$, and that with negative v_E a backward mode, $|b\rangle$. As the core thickness increases, v_E of both eigenmodes converges to zero [Fig. 1(b)], and their effective mode indices, $n_{\mathrm{eff}} = \beta/k_0$, become degenerate, as shown in Fig. 1(c). At this point, not only do the eigenvalues coalesce, but also the field profiles (see Fig. 5 in Appendix), which is a pronounced characteristic of the EP. In the symmetric *I-M-I* waveguide ($\varepsilon_{I1} = \varepsilon_{I2}$), the group velocity of each eigenmode $\partial\omega/\partial\beta$ and the geometry-related parameter $\partial\alpha/\partial\beta$ can be derived from dispersion Eq. (1):

$$\frac{\partial\omega}{\partial\beta} = cn_{\mathrm{eff}}\frac{2-\alpha\kappa_{\mathrm{I}}[1-(n_{\mathrm{eff}}^2/n_{I\text{-}M}^2)]}{2-\alpha\varepsilon_M\kappa_{\mathrm{I}}[1-(n_{\mathrm{eff}}^2/n_{I\text{-}M}^2)]}, \tag{2}$$

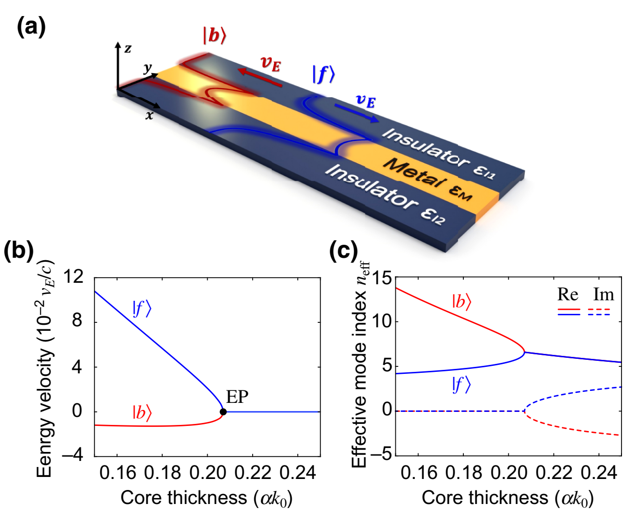

FIG. 1. Exceptional point in the lossless *I-M-I* waveguide. (a) Schematic of the *I-M-I* plasmonic waveguide with H_z field profile of the two propagating eigenmodes with positive ($|f\rangle$; blue) and negative ($|b\rangle$; red) energy velocity. (b) Energy velocity and (c) effective mode index of the eigenmodes in the lossless waveguide, showing the onset of the EP regime at $\alpha_{\mathrm{EP}}k_0 \approx 0.207$; $\varepsilon_{I1} = \varepsilon_{I2} = 12, \varepsilon_M = -10$.

$$\frac{\partial \alpha}{\partial \beta} = k_0 n_{\text{eff}} \frac{2 - \alpha\kappa_{\text{I}}[1 - (n_{\text{eff}}^2/n_{I\text{-}M}^2)]}{\kappa_{\text{I}}\kappa_M^2[1 - (n_{\text{eff}}^2/n_{I\text{-}M}^2)]}, \tag{3}$$

where c is the speed of light. Notably, the coalescence of the eigenmodes leads to the formation of an EP, where the group velocity $\partial\omega/\partial\beta$ and the geometry-related parameter $\partial\alpha/\partial\beta$ simultaneously vanish for both eigenmodes at the critical core thickness $\alpha_{\text{EP}} = 2\kappa_{\text{I}}^{-1}[1 - (n_{\text{eff}}^2/n_{I\text{-}M}^2)]^{-1}$. Interestingly, it has only been recently highlighted that the eigenmodes' coalescence at exceptional points and the vanishing group velocity are theoretically linked in systems with a certain distribution of gain and loss [5].

The manifestation of an EP in the I-M-I waveguide can be understood by investigating the properties of the system's optical Hamiltonian $H = \begin{pmatrix} a & b \\ c & d \end{pmatrix}$, where a and d correspond to the eigenvalues of the two isolated I-M interface modes. In the regime when $\rho_{1,2} > 1$ and $\gamma_{1,2} = 0$, each isolated I-M interface supports only a nonpropagating leaky mode with purely imaginary $\beta_{I\text{-}M}$ [21,22], which satisfies the mathematical condition to form an EP, as $a - d$ is purely imaginary.

In the I-M-I waveguide with a finite core thickness, the coupling between the two I-M interfaces (b and c terms in the optical Hamiltonian) results in a pair of eigenmodes that are no longer leaky, but confined in the transverse direction. In weak coupling regime ($\alpha > \alpha_{\text{EP}}$), the effective indices of eigenmodes are a pair of complex conjugates, corresponding to a system with balanced gain and loss, although the considered plasmonic modes do not experience any actual energy gain or dissipation. As the metallic core gets thinner, the coupling between the two I-M interfaces grows and eventually balances out the "fictitious," or mathematical, gain-loss at $\alpha = \alpha_{\text{EP}}$, allowing for the two modes to coalesce at the EP with a real effective index. As the core thickness further decreases ($\alpha < \alpha_{\text{EP}}$), the coupling strength outweighs the fictitious gain-loss and the effective indices of the propagating modes $|f\rangle$ and $|b\rangle$ divert from each other, as shown in Fig. 1(c), similar to the case of a PT-symmetric system [10].

The behavior of $|f\rangle$ and $|b\rangle$ modes in the I-M-I waveguide is nearly identical to that of the modes in coupled waveguide systems with balanced gain and loss, except for two key differences. First, the energy flux ($\int S_x dy$) of both modes converges to zero at the α_{EP}, and the modes are nonpropagating when $\alpha > \alpha_{\text{EP}}$. Notably, in conventional gain-loss balanced systems, the eigenmodes still have nonzero energy velocities, even beyond the EP where the effective indices of the modes become complex. Consequently, we speculate that the encircling of the EP in the parametric space of the optical Hamiltonian, as exploited in many previous studies [25–27], would not be possible in the lossless I-M-I configuration. Second, more importantly, the I-M-I plasmonic waveguide with purely real permittivities can be considered a closed system without energy exchange with the environment, since both $|f\rangle$ and $|b\rangle$ have zero radiation loss, as their fields decay exponentially further from the interfaces (Fig. 5 in Appendix). The absence of radiative loss is consistent with high effective indices of the eigenmodes, which cannot couple to the radiative modes without an additional phase-matching mechanism. We note that special cases of I-M-I waveguides also support the low-index long-range surface plasmons that couple to radiative modes [28]; however, this is not the case in this study.

At first glance, it may sound contradictory that a Hamiltonian of a system without energy gain or loss could be non-Hermitian. However, we point out that the Hermiticity of optical Hamiltonians for guided modes in waveguides does not require energy conservation, since the eigenvalues are propagation constants of the optical modes [2]. Accordingly, the spatial coordinate along the axis of propagation (in our case, the x axis) in the paraxial equation plays the role of time t in the Schrodinger equation [10]. In typical optical systems, these differences are not pronounced, as the phase and energy of the modes propagate in a similar manner. In contrast, the phase and energy propagations in our system are completely different. In the weak coupling regime ($\alpha > \alpha_{\text{EP}}$), the effective indices of the modes are a pair of complex conjugates, whereas the energy velocity vanishes. In the strong coupling regime ($\alpha < \alpha_{\text{EP}}$), the effective indices of the modes are real numbers with the same sign, whereas the energy velocities of $|f\rangle$ and $|b\rangle$ have opposite signs. As a result, the behavior of the mode indices and the eigenvalues of the optical Hamiltonian are mathematically equivalent to that of a pair of waveguides with balanced gain and loss, allowing an EP to be formed, even in a structure without energy gain or loss.

B. Exceptional points in a symmetric *I*-*M*-*I* waveguide

We proceed with analyzing the properties of the EP as material loss and gain are introduced in a balanced manner (i.e., $\gamma = \pm\gamma_1 = \mp\gamma_2$) to the symmetric I-M-I waveguide with $\rho_1 = \rho_2 = \rho > 1$. Figures 2(a) and 2(b) show how n_{eff} and α_{EP} vary, depending on the system parameters, respectively, when ε_M is fixed to -10. At a constant ρ, we observe that EP occurs at smaller core thicknesses as $|\gamma|$ increases. With a fixed $|\gamma|$, α_{EP} also decreases with increasing ρ, akin to balancing out larger gain and loss from the individual modes' indices with stronger coupling in a PT-symmetric coupled waveguide system. When nonzero γ is introduced, the energy velocities of the modes beyond the EP ($\alpha > \alpha_{\text{EP}}$) are no longer zero, but actually convey energy along the propagation direction, as in the conventional coupled waveguide system with balanced gain and loss.

On the other hand, when ρ is sufficiently smaller than one and $\gamma = 0$, each I-M interface supports propagating surface plasmons with real $\beta_{I\text{-}M}$. The I-M-I waveguide

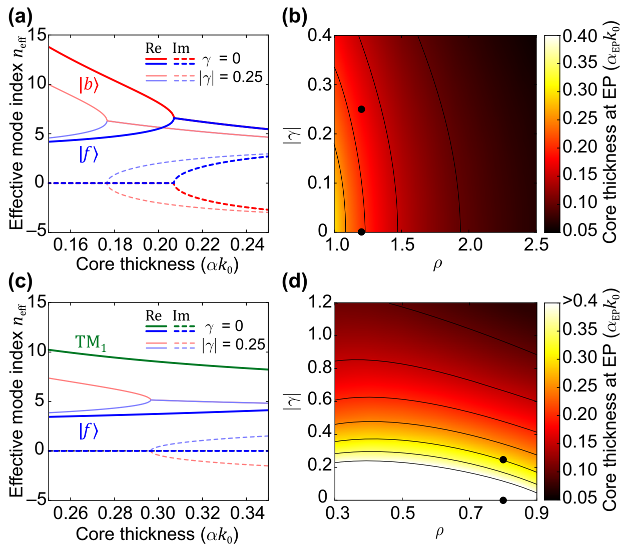

FIG. 2. Analysis of EP regime in symmetric *I-M-I* waveguide with and without material gain and loss. (a) Effective mode index of eigenmodes with and without material gain-loss $\gamma = \mathrm{Im}[\varepsilon_I]/\mathrm{Re}[\varepsilon_I]$ when $\mathrm{Re}[\varepsilon_I] = 12, \varepsilon_M = -10$ ($\rho > 1$), showing the constant presence of the EP at coalescence of the eigenmodes with antiparallel energy velocity. (b) Core thickness corresponding to the onset of the EP as a function of γ and ρ when $\rho > 1$; black dots indicate system parameters in (a). (c) Effective mode index of eigenmodes with and without γ when $\mathrm{Re}[\varepsilon_I] = 8, \varepsilon_M = -10$ ($\rho < 1$): one even ($|f\rangle$; blue) and one odd (TM_1; green) eigenmode is supported by the structure, unless nonzero γ is introduced, forbidding the existence of EP in the lossless case. (d) Same as in (b), when $\rho < 1$, showing divergence of α_{EP} when $\gamma \to 0$; black dots indicate system parameters in (c).

supports one even (TM_0) and one odd (TM_1) mode [Fig. 2(c)], both having real propagation constants and positive energy velocity. These two eigenmodes cannot become degenerate because of different field parity. In this case, EP can be retrieved only with symmetrically introduced gain and loss [Fig. 2(c)], which would correspond to a conventional *PT*-symmetric system [10,11,29]. Therefore, α_{EP} diverges as $\gamma \to 0$ [Fig. 2(d)], and EPs are exhibited only if $|\gamma| > 0$. Here, again, α_{EP} decreases with increasing $|\gamma|$ due to a stronger coupling being required to balance out the increased gain-loss. The dependence of α_{EP} on ρ may seem somewhat nontrivial, but can be explained using similar reasoning of coupling balancing out gain and loss [10].

Interestingly, we find that the dispersion of lossless *I-M-I* waveguides possesses nontrivial fine structures for transitional cases at $\rho \approx 1$, as summarized in Fig. 3. The previously discussed case with$\rho \geq 1$ (at $\gamma = 0$) is shown in Fig. 3(a). In Fig. 3(b), we plot the eigenvalues from Fig. 3(a) as a function of α on a complex plane to clearly show their dynamics near the EP (shown by the red dot) as α transitions through α_{EP}. The arrows indicate the evolution of eigenmodes from propagating (solid arrows) to nonpropagating (dashed arrows) as the core thickness increases. When ρ becomes slightly less than one, two additional modes of different parity with positive energy velocity enter the solution space [Fig. 3(c)]. Among the TM_0 modes, the backward mode, $|b\rangle$ (red), coalesces with each of the two forward modes, $|f_1\rangle$ and $|f_2\rangle$ (blue), so that two separate EPs are formed in the system, as demonstrated in Fig. 3(d) on a complex plane. As we further decrease ρ, the two separate EPs merge at the same α_{EP}, as shown in Fig. 3(e). Then, three TM_0 eigenmodes coalesce at a single α_{EP}, forming a third-order EP [encircled red dot in Fig. 3(f)]. The value of ρ associated with a third-order EP made from the fundamental modes is the minimum possible for a given system, and no EPs are present if ρ is smaller than this value, unless actual gain and loss are introduced into the system, as shown in Figs. 3(g) and 3(h).

We note that, in a conventional photonic system, three subsystems with propagating modes are required to form a third-order EP. The excitation and simultaneous coalescence of three eigenmodes is not a trivial task, and hence, complicated geometries are suggested to form a third-order EP [13,30]. Here, however, we show that a third-order EP can be formed, even in a simple *I-M-I* waveguide.

The intersection angle between the eigenvalue traces on the complex plane represents the degeneracy order at the EP. If we assume a system with n eigenmodes, it can be described by an $n \times n$ Hamiltonian. In the vicinity of the nth order EP, where the Hamiltonian solutions can be approximated as straight lines [Figs. 3(b), 3(d), 3(f) and 3(h)], the Hamiltonian can be written as an nth order equation with n degenerate roots near the EP, as follows [31]:

$$(\lambda_m - \beta_{\mathrm{EP}})^n = r^n e^{in\theta_m} = \xi, \tag{4}$$

where λ_m are the eigenvalues of the Hamiltonian, β_{EP} is the degenerate eigenvalue at the EP, $\mathrm{Re}(\xi) = r^n$, and $\theta_m = 2\pi m/n$ ($m = 0,\ 1,\ 2,\ \cdots,\ n-1$). Then, the eigenvalues of the Hamiltonian are given by $\lambda_m = \beta_{\mathrm{EP}} + re^{i\theta_m}$, and thus, the parameter ξ determines whether the eigenvalues are real or complex and is zero at the EP. From the perspective of the coupled mode theory in a conventional *PT*-symmetric structure ($n = 2$), for example, $\xi = |\kappa_c|^2 - |\mathrm{Im}(\beta_{\mathrm{sub}})|^2$, where κ_c is the coupling coefficient and β_{sub} is the propagation constant of an eigenmode of the subsystem. In the real eigenvalue regime, the value of ξ is positive, and thus, all eigenvalue traces intersect at the EP at a constant angle of $\varphi_n = \pi/n = \theta_m/2m$. In the complex eigenvalue regime (or *PT*-broken regime), ξ is negative, which can be treated as a positive real value with $\theta_m = (2m+1)\pi/n$. Therefore, upon the transition through the EP, the eigenvalue traces intersect at the EP at a constant angle of $\varphi_n = \pi/n = \theta_m/2m$, as we show in Figs. 3(b), 3(d) and 3(f).

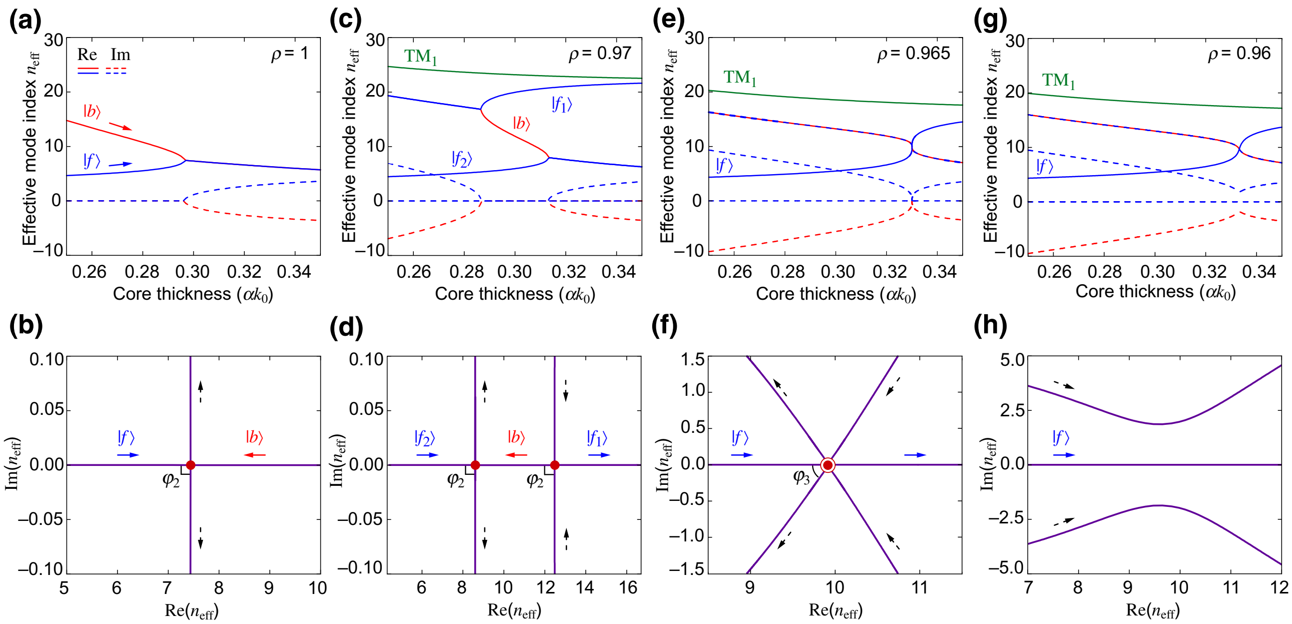

FIG. 3. Formation of third-order exceptional point in lossless symmetric I-M-I waveguide. Top row: effective indices of the eigenmodes as a function of core thickness for systems with different ρ ($\varepsilon_M = -10$): (a) $\varepsilon_I = 10$, (c) $\varepsilon_I = 9.7$, (e) $\varepsilon_I \approx 9.65$, and (g) $\varepsilon_I = 9.6$. Bottom row: same effective indices plotted on a complex plane. (b),(d) Second-order EPs (red dots) corresponding to (a), (c), respectively. (f) Coalescence dynamics of three eigenmodes shown in (e) forming the third-order EP. No EPs exist for smaller ρ, as demonstrated in (g) and (h). Arrows indicate evolution of the effective index of propagating (solid) and nonpropagating (dashed) eigenmodes as core thickness increases. Intersection angle $\varphi_n = \pi/n$ corresponds to degeneracy order n.

C. Exceptional points in an asymmetric *I*-*M*-*I* waveguide

Finally, we consider I-M-I structures with broken P symmetry ($\varepsilon_{I1} \neq \varepsilon_{I2}$). Since $a - d$ stays purely imaginary if $\rho_{1,2} > 1$ and $\gamma_{1,2} = 0$, P symmetry is dispensable for manifestation of EPs in asymmetric lossless I-M-I waveguides. To illustrate the constant presence of the EP regime, we calculate $\alpha_{\rm EP}$ for the asymmetric I-M-I waveguide as a function of ρ_1 and ρ_2, as shown in Fig. 4(a), while maintaining $\varepsilon_M = -10$. Similar to the previous cases, $\alpha_{\rm EP}$ decreases as either ρ_1 or ρ_2 increases. In contrast, the system with broken P symmetry and $\gamma_{1,2} \neq 0$ requires a specific ratio of gain and loss of $\pm\gamma_{2,\rm EP}/\mp\gamma_{1,\rm EP}$ to access the EP regime, depending on the values of $\rho_{1,2}$. We calculate the required ratio of $-\gamma_{2,\rm EP}/\gamma_{1,\rm EP}$ as a function of $\rho_{1,2}$, confirming the consistent presence of EPs [Fig. 4(b)].

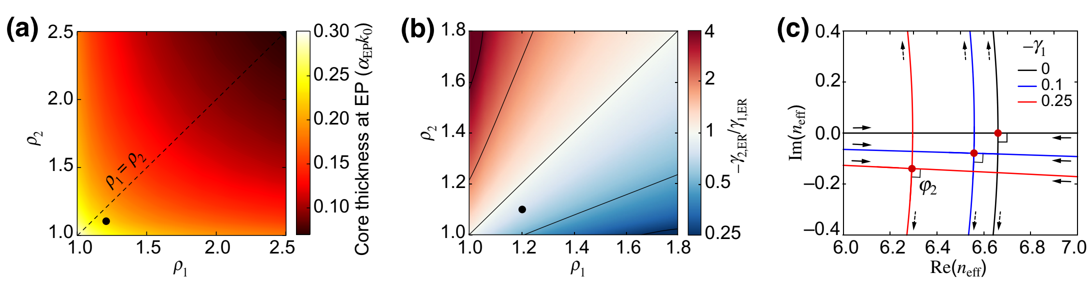

FIG. 4. Analysis of the exceptional point regime in asymmetric I-M-I waveguide with and without material gain and loss. (a) Core thickness $\alpha_{\rm EP}k_0$ corresponding to the EP regime, when $\rho_{1,2} > 1$ and $\gamma_j = 0$. (b) Specific ratio between material gain-loss in two insulator layers ($-\gamma_{2,\rm EP}/\gamma_{1,\rm EP}$) required for the manifestation of EP as a function of $\rho_{1,2}$. (c) Complex plane plot of effective indices of waveguide eigenmodes, showing second-order EPs (red dots) formed when $\gamma_j = 0$ (black lines) and$\gamma_j \neq 0$ (red and blue lines); Re[ε_{I1}]= 12, Re[ε_{I2}] = 11, and $\varepsilon_M = -10$, as indicated by the black dot in (a) and (b). Arrows indicate evolution of the eigenmodes' effective indices before (solid) and after (dashed) onset of the EP regime as core thickness increases.

We note that the condition $\rho_{1,2} > 1$ must be satisfied; otherwise, EPs cannot be formed, even if gain and loss are introduced.

The complex-plane trace of the eigenvalues in the asymmetric structure near the EP regime is shown in Fig. 4(c). Interestingly, the eigenvalues of the system with both P and T symmetries broken are not required to be real to manifest the EP in the complex eigenvalue regime. The unbalanced gain and loss are reflected as the rotation of the eigenvalue traces near the EP, while the intersection angle $\varphi_2 = \pi/2$ is preserved. We note that this type of EP has been widely studied in other photonic systems, including passive PT symmetry with asymmetric material [8] or radiative losses [9].

III. CONCLUSIONS

We demonstrate the emergence of EPs in an I-M-I plasmonic waveguide possessing neither gain nor loss, including the case when P symmetry is broken. The subtle distinction between the Schrodinger equation and the optical paraxial equation for waveguides allows an optical Hamiltonian to be non-Hermitian without energy exchange with the environment, when materials with negative permittivities are introduced to the system, and thus, the directions of energy and phase propagation are no longer parallel. Furthermore, we show the possibility of combining EPs to generate a higher-order EP in a simple plasmonic structure. Generally, the necessity of simultaneously exciting three eigenmodes that coalesce in the EP regime to access higher-order EPs in photonic systems limit the practicality. Our study suggests that the generation of a third-order EP is possible in a simple I-M-I structure, which relaxes the geometrical and material restrictions and gives an insight into generating higher-order EPs. Finally, we analyze cases with gain and loss in the system, showing that achieving an EP in the system with broken P symmetry requires an asymmetric gain and loss profile. We speculate that our findings are not limited only to plasmonic systems, but also extend to a wider class of photonic systems with decoupled phase and energy propagation.

ACKNOWLEDGMENTS

This work was supported by the National Research Foundation of Korea (NRF) funded by Ministry of Science and ICT (Grants No. 2017R1E1A1A01074323 and No. 2016M3D1A1900038). S.Y.M. and S.G.M. acknowledge support from the NRF Young Researchers program funded by Ministry of Science and ICT (Grant No. 2019R1C1C1011131).

APPENDIX: MAGNETIC FIELD PROFILE OF THE EIGENMODES IN AN *I-M-I* WAVEGUIDE

When $\alpha < \alpha_{EP}$, the waveguide supports two propagating TM_0 eigenmodes with one $|f\rangle$ and one $|b\rangle$ mode (see Fig. 1(c) for details). In terms of the governing magnetic field H_z, the eigenmodes have nonzero Re$[H_z]$, while Im$[H_z] = 0$, as shown in Fig. 5(a). As the core thickness increases, the two eigenmodes (Fig. 5(a), blue and red) coalesce at the EP when $\alpha = \alpha_{EP}$ (Fig. 5(a), black), still having a real effective index. When $\alpha > \alpha_{EP}$, the two eigenmodes split again, with their effective indices being a pair of complex conjugates, which is reflected in the field profile (Fig. 5(b)). This demonstrates that the system always supports two eigenmodes except for the EP.

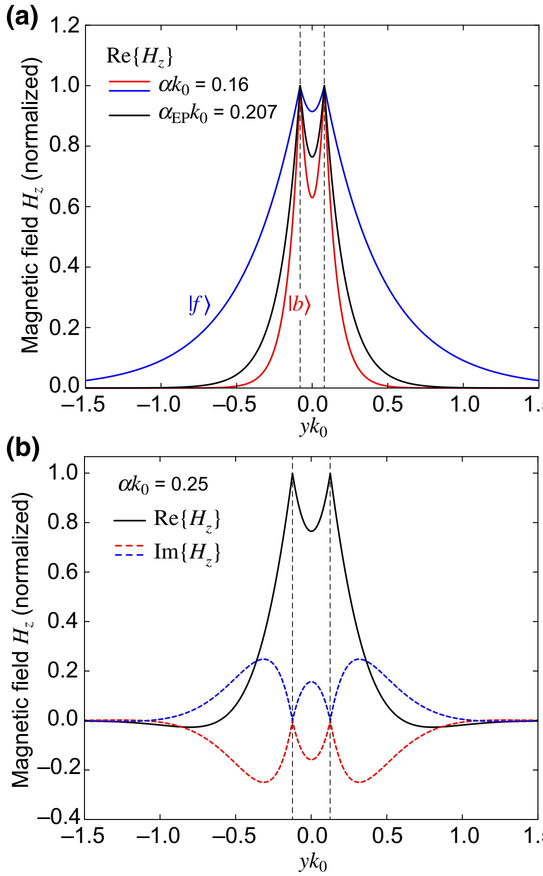

FIG. 5. Magnetic field profile of TM eigenmodes in lossless I-M-I waveguide. (a) Purely real magnetic field of propagating eigenmodes before onset of the EP regime (blue, forward mode; red, backward mode) and coalescent field profiles of both modes at EP (black). (b) Real and imaginary parts of the magnetic field for nonpropagating eigenmodes after onset of the EP regime. $\varepsilon_I = 12, \varepsilon_M = -10$ and dashed lines indicate location of I-M interfaces.

[1] C. M. Bender and S. Boettcher, Real Spectra in non-Hermitian Hamiltonians Having PT Symmetry, Phys. Rev. Lett. **80**, 5243 (1998).

[2] S. Longhi, Quantum-optical analogies using photonic structures, Laser Photonics Rev. **3**, 243 (2009).

[3] L. Feng, Z. J. Wong, R.-M. Ma, Y. Wang, and X. Zhang, Single-mode laser by parity-time symmetry breaking, Science **346**, 972 (2014).
[4] H. Hodaei, M.-A. Miri, M. Heinrich, D. N. Christodoulides, and M. Khajavikhan, Parity-time–symmetric microring lasers, Science **346**, 975 (2014).
[5] T. Goldzak, A. A. Mailybaev, and N. Moiseyev, Light Stops at Exceptional Points, Phys. Rev. Lett. **120**, 013901 (2018).
[6] Z. Lin, H. Ramezani, T. Eichelkraut, T. Kottos, H. Cao, and D. N. Christodoulides, Unidirectional Invisibility Induced by PT-Symmetric Periodic Structures, Phys. Rev. Lett. **106**, 213901 (2011).
[7] D. L. Sounas, R. Fleury, and A. Alù, Unidirectional Cloaking Based on Metasurfaces with Balanced Loss and Gain, Phys. Rev. Appl. **4**, 014005 (2015).
[8] A. Guo, G. J. Salamo, D. Duchesne, R. Morandotti, M. Volatier-Ravat, V. Aimez, G. A. Siviloglou, and D. N. Christodoulides, Observation of PT-Symmetry Breaking in Complex Optical Potentials, Phys. Rev. Lett. **103**, 093902 (2009).
[9] B. Zhen, C. W. Hsu, Y. Igarashi, L. Lu, I. Kaminer, A. Pick, S.-L. Chua, J. D. Joannopoulos, and M. Soljačić, Spawning rings of exceptional points out of Dirac cones, Nature **525**, 354 (2015).
[10] Ş Özdemir, S. Rotter, F. Nori, and L. Yang, Parity-time symmetry and exceptional points in photonics, Nat. Mater. **18**, 783 (2019).
[11] A. A. Zyablovsky, A. P. Vinogradov, A. A. Pukhov, A. V. Dorofeenko, and A. A. Lisyansky, PT-symmetry in optics, Phys.-Usp **57**, 1063 (2014).
[12] W. Chen, ŞK Özdemir, G. Zhao, J. Wiersig, and L. Yang, Exceptional points enhance sensing in an optical microcavity, Nature **548**, 192 (2017).
[13] H. Hodaei, A. U. Hassan, S. Wittek, H. Garcia-Gracia, R. El-Ganainy, D. N. Christodoulides, and M. Khajavikhan, Enhanced sensitivity at higher-order exceptional points, Nature **548**, 187 (2017).
[14] S. Wang, B. Hou, W. Lu, Y. Chen, Z. Q. Zhang, and C. T. Chan, Arbitrary order exceptional point induced by photonic spin–orbit interaction in coupled resonators, Nat. Commun. **10**, 1 (2019).
[15] N. Moiseyev, *Non-Hermitian Quantum Mechanics* (Cambridge University Press, Cambridge, England, 2011).
[16] W.-P. Huang, Coupled-mode theory for optical waveguides: An overview, J. Opt. Soc. Am. A **11**, 963 (1994).
[17] C. E. Rüter, K. G. Makris, R. El-Ganainy, D. N. Christodoulides, M. Segev, and D. Kip, Observation of parity–time symmetry in optics, Nat. Phys. **6**, 192 (2010).
[18] L. Chang, X. Jiang, S. Hua, C. Yang, J. Wen, L. Jiang, G. Li, G. Wang, and M. Xiao, Parity–time symmetry and variable optical isolation in active–passive-coupled microresonators, Nat. Photonics **8**, 524 (2014).
[19] F. Yang, Y.-C. Liu, and L. You, Anti-PT symmetry in dissipatively coupled optical systems, Phys. Rev. A **96**, 053845 (2017).
[20] Y. Choi, C. Hahn, J. W. Yoon, and S. H. Song, Observation of an anti-PT-symmetric exceptional point and energy-difference conserving dynamics in electrical circuit resonators, Nat. Commun. **9**, 1 (2018).
[21] P. A. D. Gonçalves and N. M. R. Peres, *An Introduction to Graphene Plasmonics* (World Scientific, Singapore, 2016).
[22] S. A. Maier, *Plasmonics: Fundamentals and Applications* (Springer Science & Business Media, New York, 2007).
[23] M. S. Jang and H. Atwater, Plasmonic Rainbow Trapping Structures for Light Localization and Spectrum Splitting, Phys. Rev. Lett. **107**, 207401 (2011).
[24] J. Park, S. Kim, J. Lee, S. G. Menabde, and M. S. Jang, Ultimate Light Trapping in a Free-Form Plasmonic Waveguide, Phys. Rev. Appl. **12**, 024030 (2019).
[25] J. Doppler, A. A. Mailybaev, J. Böhm, U. Kuhl, A. Girschik, F. Libisch, T. J. Milburn, P. Rabl, N. Moiseyev, and S. Rotter, Dynamically encircling an exceptional point for asymmetric mode switching, Nature **537**, 76 (2016).
[26] A. U. Hassan, B. Zhen, M. Soljačić, M. Khajavikhan, and D. N. Christodoulides, Dynamically Encircling Exceptional Points: Exact Evolution and Polarization State Conversion, Phys. Rev. Lett. **118**, 093002 (2017).
[27] J. W. Yoon, Y. Choi, C. Hahn, G. Kim, S. H. Song, K.-Y. Yang, J. Y. Lee, Y. Kim, C. S. Lee, J. K. Shin, H.-S. Lee, and P. Berini, Time-asymmetric loop around an exceptional point over the full optical communications band, Nature **562**, 86 (2018).
[28] P. Berini, Long-range surface plasmon polaritons, Adv. Opt. Photon. **1**, 484 (2009).
[29] R. El-Ganainy, K. G. Makris, M. Khajavikhan, Z. H. Musslimani, S. Rotter, and D. N. Christodoulides, Non-Hermitian physics and PT symmetry, Nat. Phys. **14**, 11 (2018).
[30] Z. Lin, A. Pick, M. Lončar, and A. W. Rodriguez, Enhanced Spontaneous Emission at Third-Order Dirac Exceptional Points in Inverse-Designed Photonic Crystals, Phys. Rev. Lett. **117**, 107402 (2016).
[31] T. Kato, *Perturbation Theory for Linear Operators* (Springer Science & Business Media, New York, 1966).